Hindawi Publishing Corporation
Journal of Chemistry
Volume 2014, Article ID 921863, 16 pages
http://dx.doi.org/10.1155/2014/921863

Research Article

Chemical Feature-Based Molecular Modeling of Urotensin-II Receptor Antagonists: Generation of Predictive Pharmacophore Model for Early Drug Discovery

Anubhuti Pandey,[1] Sarvesh Kumar Paliwal,[1] and Shailendra Kumar Paliwal[2]

[1] *Department of Pharmacy, Banasthali University, Rajasthan 304022, India*
[2] *Department of Pharmacy, LLRM Medical College, Meerut, Uttar Pradesh 250004, India*

Correspondence should be addressed to Anubhuti Pandey; anubhuti_pandey@ymail.com

Received 6 May 2013; Revised 19 November 2013; Accepted 3 December 2013; Published 3 February 2014

Academic Editor: Georgia Melagraki

For a series of 35 piperazino-phthalimide and piperazino-isoindolinone based urotensin-II receptor (UT) antagonists, a thoroughly validated 3D pharmacophore model has been developed, consisting of four chemical features: one hydrogen bond acceptor lipid (HBA_L), one hydrophobe (HY), and two ring aromatic (RA). Multiple validation techniques like CatScramble, test set prediction, and mapping analysis of advanced known antagonists have been employed to check the predictive power and robustness of the developed model. The results demonstrate that the best model, Hypo 1, shows a correlation (r) of 0.902, a root mean square deviation (RMSD) of 0.886, and the cost difference of 39.69 bits. The model obtained is highly predictive with good correlation values for both internal ($r^2 = 0.707$) as well as external ($r^2 = 0.614$) test set compounds. Moreover, the pharmacophore model has been used as a 3D query for virtual screening which served to detect prospective new lead compounds which can be further optimized as UT antagonists with potential for treatment of cardiovascular diseases.

1. Introduction

The role of urotensin-II (U-II) cyclic peptides and their cell-surface receptor in cardiovascular regulation is very well established. Human U-II is considered to be the most potent vasoconstrictor known, approximately 10 times more potent than endothelin-1 [1]. It is an 11 amino acid cyclic peptide, expressed mainly in the blood vessels, heart, liver, kidney, skeletal muscle, and lung [2]. Urotensin II receptor (UT) is a Gq protein coupled receptor originally identified as the orphan GPR14 receptor by Ames et al. in 1999 [1]. The utility of UT antagonists as potential therapeutic agents in treating atherosclerosis, hypertension, and metabolic syndrome has been suggested by a wide range of studies in animal models [3]. Therefore a UT antagonist may have enormous therapeutic potential in the treatment of hypertension and cardiac and renal failure.

Palosuran (ACT-058362), the only UT antagonist drug candidate, when administered intravenously, protected against renal ischemia in a rat model [4]. However, clinical studies of palosuran were ceased in May 2005 due to lack of efficacy in humans [5]. Therefore it is the need of the hour that new UT antagonists should be developed for the treatment of cardiovascular and renal diseases.

Pharmacophore modeling has proven extremely successful in the drug design process by demonstrating structure-activity relationships [6–9]. A good pharmacophore model collects important common chemical features of molecules distributed in the 3D space and provides a rational hypothetical conformation responsible for activity. Thus, it provides the essential structural requirements for the ligands to have good interactions at the target, which may also prove helpful in the identification of new active and specific inhibitors [10, 11].

Earlier, Lescot et al. in 2007 performed 3D pharmacophore-based studies on a set of diverse UT antagonists including benzazepine, biphenylcarboxamide, quinoline, sulfonamide, indole, and quinolone derivatives. They depicted two distinctively different models based on a common feature alignment approach comprising two aromatic rings, one

hydrophobic group, a basic amine centre, and a hydrogen bond acceptor, each with a different spatial distribution, thus suggesting a lack of convergence between the considered antagonist ligands [12, 13]. In view of this we envisaged to undertake QSAR based pharmacophore modeling of UT antagonists taking into account both chemical structures as well as activity data of a series of compounds. In the present study, a 3D QSAR based pharmacophore modeling was employed to understand the structural features that are common in the piperazino-phthalimide and piperazino-isoindolinone based UT antagonists [14]. Our pharmacophore model consists of one hydrogen bond acceptor lipid (HBA_L) and one hydrophobic (HY) and two ring aromatic (RA) features. The model has been thoroughly validated using Fisher's cross validation [15] and activity prediction of internal test set as well as external data set of compounds. Also, the pharmacophore model has been used as a 3D query for virtual screening which has detected potential new compounds which can be further optimized as UT antagonists.

2. Experimental

2.1. Data Set. A series of UT antagonists based on piperazino-phthalimide and piperazino-isoindolinone groups were taken from the literature [14] (Table 1). The basic requirements of training set selection were followed; that is, a minimum of 16 structurally diverse compounds should be selected to avoid any chance of correlation and the activity data should have a range of 3–5 orders of magnitude. These compounds covered a wide range of UT inhibition activity from 1 nM to 65000 nM represented as rat FLIPR IC_{50} values. 35 compounds were selected to construct the training set. Excluding the training set compounds, the remaining compounds were used as test set to evaluate the efficiency of the pharmacophore model.

All structures were built using ChemDraw Ultra 8.0 (Cambridge Soft Corp., Cambridge, MA) and imported to Accelry's Discovery Studio 2.0 (DS 2.0, Accelrys Inc., San Diego, CA) window. Their energies were minimized to the closest local minima using the generalized CHARMM force field as implemented in DS 2.0 program.

2.2. Generation of Pharmacophores. As a prerequisite to 3D pharmacophore development, conformational models for the compounds were generated using the "best" conformer generation method [16]. The poling algorithm was used, which seeks to provide a broad coverage of conformational space with a maximum conformational energy of 20 kcal/mol above the lowest energy conformation [17]. The number of conformers generated for each compound was limited to a maximum of 250. The catalyst model treated the molecular structures as templates comprising chemical functions localized in space that binds effectively with complementary functions on the respective binding proteins. The feature mapping protocol in catalyst generated three chemical feature types, hydrogen bond acceptor lipid (HBA_L), hydrophobic (HY), and ring aromatic (RA), effectively mapping all the critical chemical features of all molecules in the data set. These three features were used to generate the pharmacophore hypotheses. The value for uncertainty was defined as 3, which represents the ratio range of uncertainty in the activity value based on the expected statistical straggling of biological data collection. Minimum points and minimum subset points were kept at the default values of 4. Based on the conformations of each compound, the HypoGen module of the catalyst was used to generate three-dimensional pharmacophore models.

2.3. Statistical Assessment of the Generated Hypotheses. The HypoGen module performs two important cost calculations (represented in bit units) that determine the success of any pharmacophore hypothesis [18]. First is the fixed cost, which represents a simple model that fits all data perfectly, while second is the null cost which presumes that there is no relationship in the data and that the experimental activities are normally distributed around their average value. A meaningful pharmacophore hypothesis may result when the difference between these two values is large; for instance, a value of 40–60 bits for the unit of cost difference implies a 75–90% probability of the correlation between experimental and predicted activities [18]. Further, total cost which sums over error cost, weight cost, and configuration cost should be close to the fixed cost, and there should be a significant difference between null and total cost. Two other parameters that also determine the quality of any pharmacophore hypothesis are the configuration cost or entropy cost, which depends on the complexity of the pharmacophore hypothesis space and should have a value <17, and the error cost, which is dependent on the root mean square differences between the estimated and the actual activities of the training set molecules. The root mean square deviation (RMSD) and the correlation coefficient represent the quality of the correlation between the estimated and the actual activity data.

The hypotheses generated by the HypoGen module have been analyzed for their statistical significance in terms of cost function analysis, correlation coefficient, and root mean square deviation.

2.4. CatScramble Validation Test. To evaluate the statistical relevance of the models, CatScramble validation has been applied. The CatScramble validation procedure is a cross validation based on Fischer's randomization test, where the biological activity data are randomized within a fixed chemical data set and the HypoGen process is initiated to explore possibilities of other hypotheses of good predictive values. For a statistically significant pharmacophoric model, the hypothesis generated prior to scrambling should be better than the rest, having lower cost values and higher correlation. The statistical significance is given by the equation of significance = $[1 - (1 + x)/y]$, where x is the total number of hypotheses having total cost lower than the most significant hypothesis and y is the number of initial HypoGen runs plus random runs.

The biological activities of the molecules in the training set were randomized and the resulting training sets were used for the HypoGen runs keeping all parameters as per the initial HypoGen calculation. In our validation test, we selected the

Table 1: Chemical structures of the piperazino-phthalimide and piperazino-isoindolinone based UT antagonists.

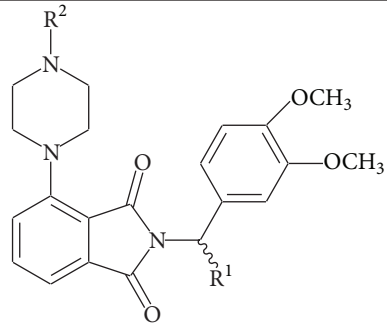

2–5[a]

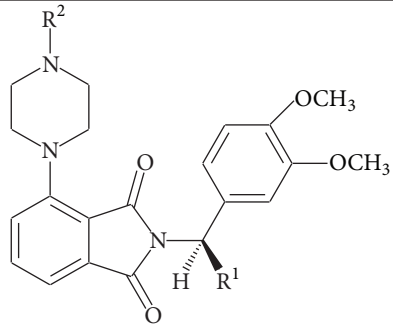

6[b]

Compound	R^1	R^2	Rat FLIPR IC_{50} (nM)
2		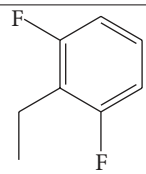	1000
3		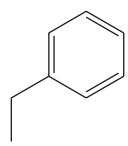	150
(R)-4		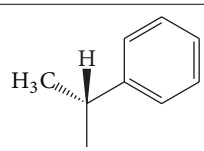	84
(S)-4		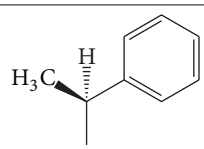	490
(R,R)-5a		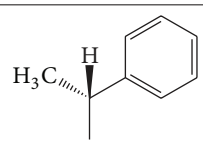	150
(R,S)-5a		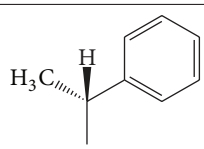	130
5b		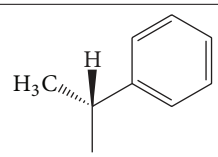	180
5c		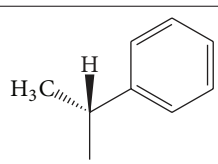	300

Table 1: Continued.

5d	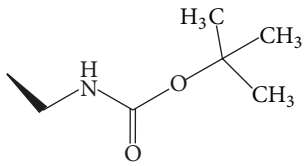	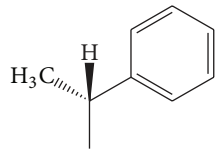	120
5e	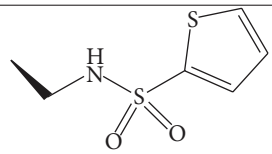	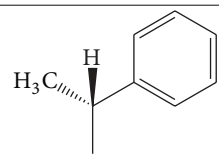	75
5f	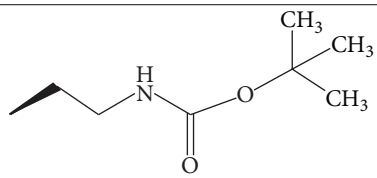	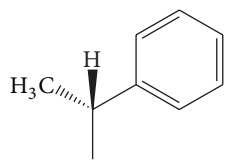	110
5g	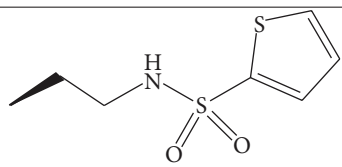	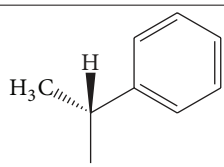	120
5h	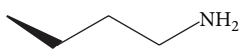	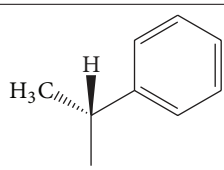	200
5i	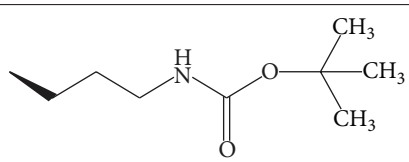	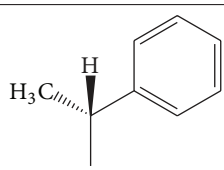	200
(R,S)-5j	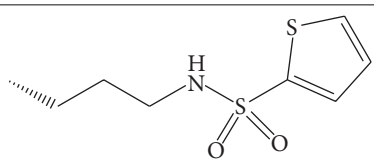	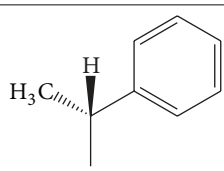	69
(R,R)-5j	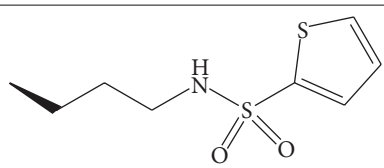	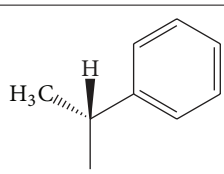	29
5l	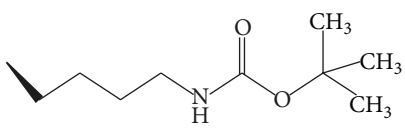	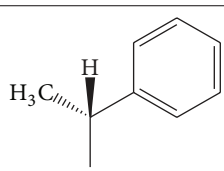	65000
5m	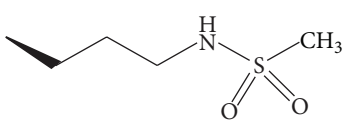	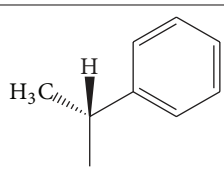	110

Table 1: Continued.

5n	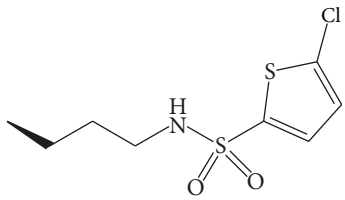	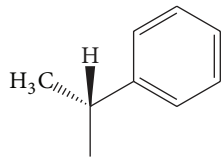	1700
6a	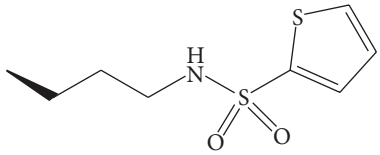		40
6b	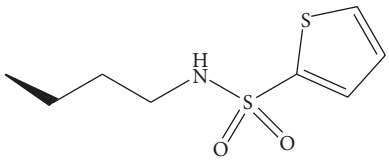		16
6c	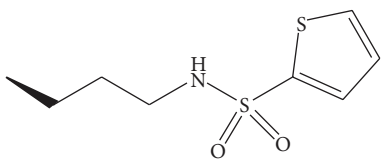	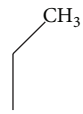	4.8
6d	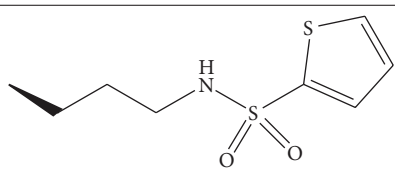	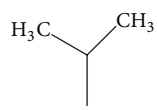	3.5
6e	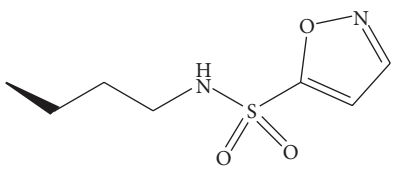	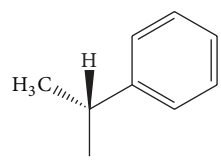	20
6f	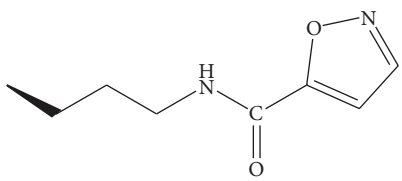	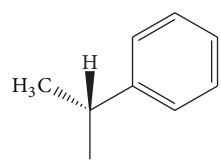	11
6g	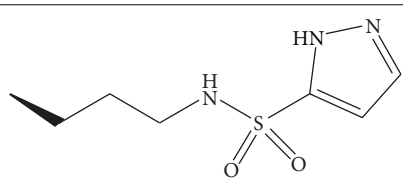	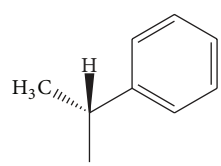	11
6h	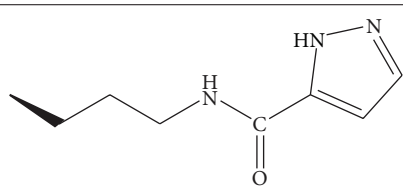	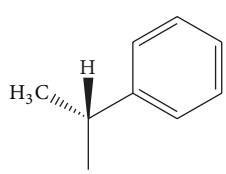	11

Table 1: Continued.

6i	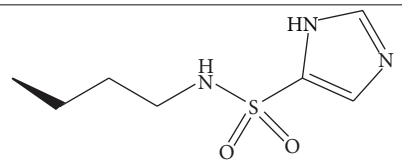	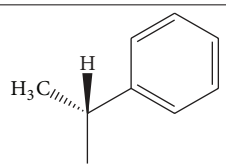	14
6j	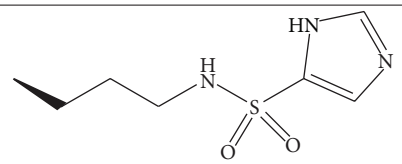	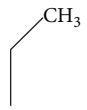	140
	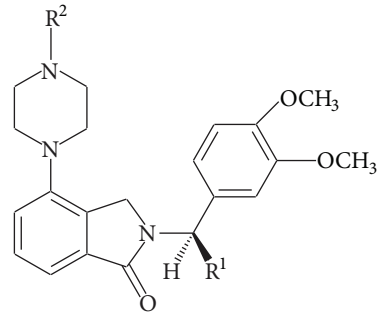 7[c]		
7a	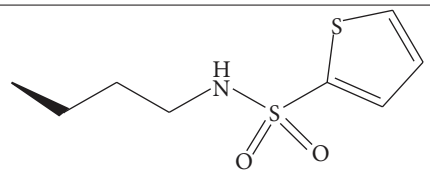	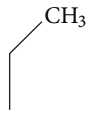	1.0
7b	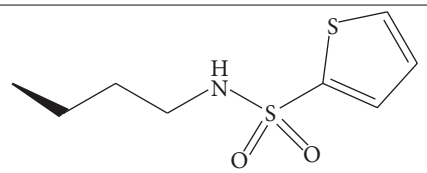	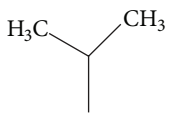	3.0
7c	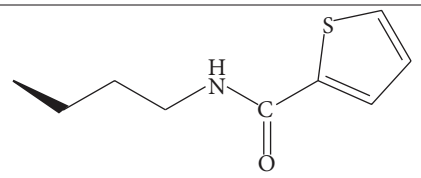	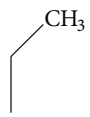	7.0
7d	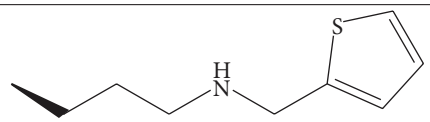	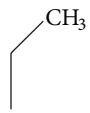	6.0
7e	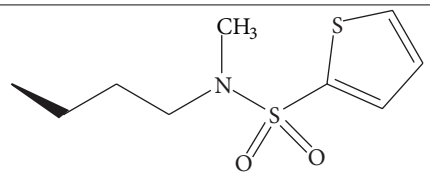	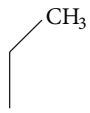	7.0
7f	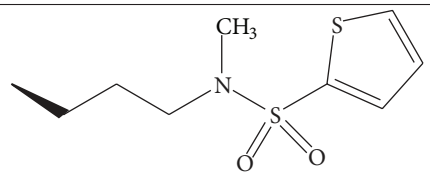		39

Table 1: Continued.

7g	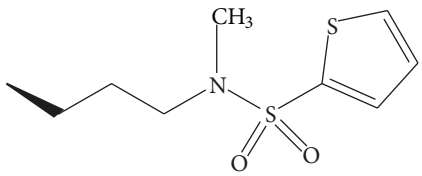		16
7h	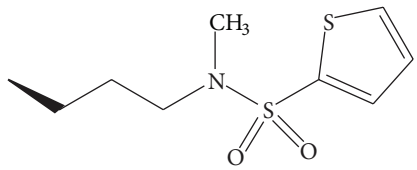	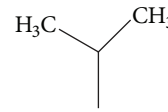	2.0
7i	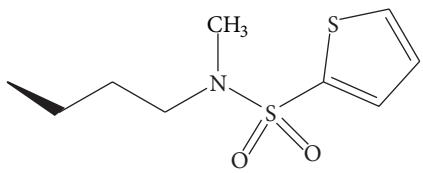		13
7j	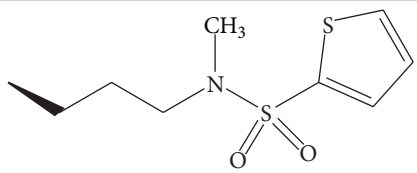	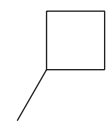	4.0
7k	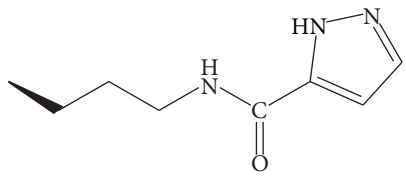	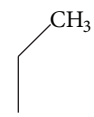	16
7l	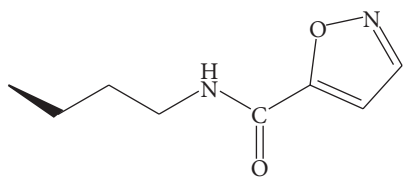	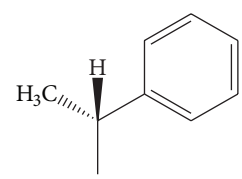	6.0
7m	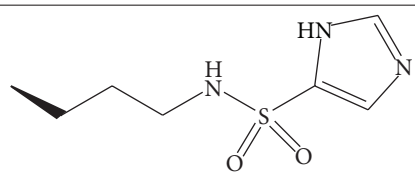	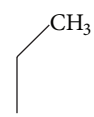	23
7n	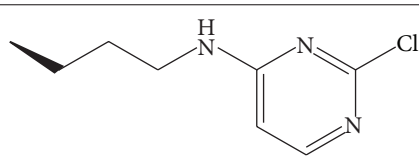	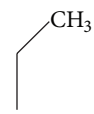	1.0
7o	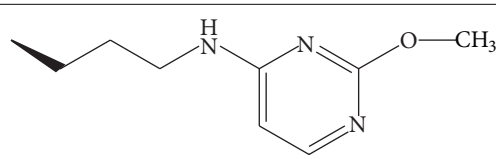	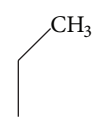	4.0

[a] Compounds 2, 3, 4, and 5a–n; [b] compounds 6a–j; [c] compounds 7a–o.

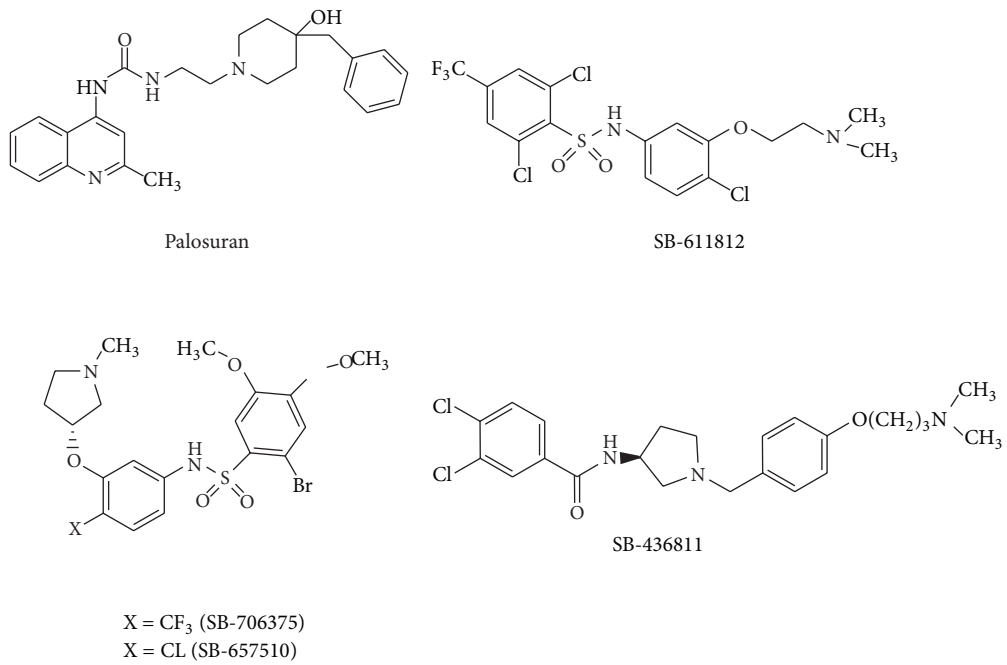

Figure 1: Advanced UT antagonists used for external validation.

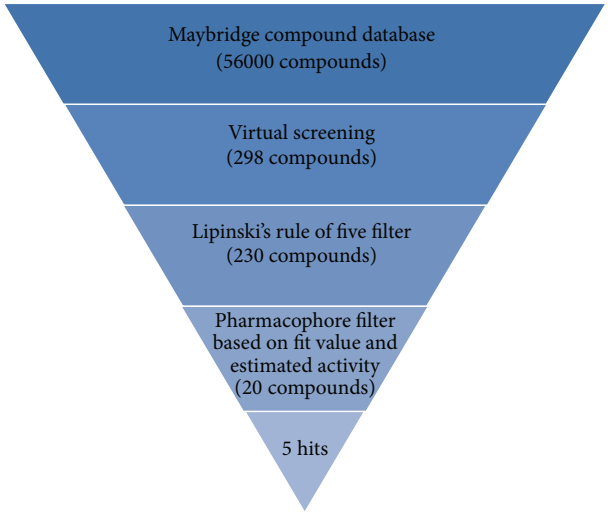

Figure 2: Schematic representation of the sequential filters used for virtual screening.

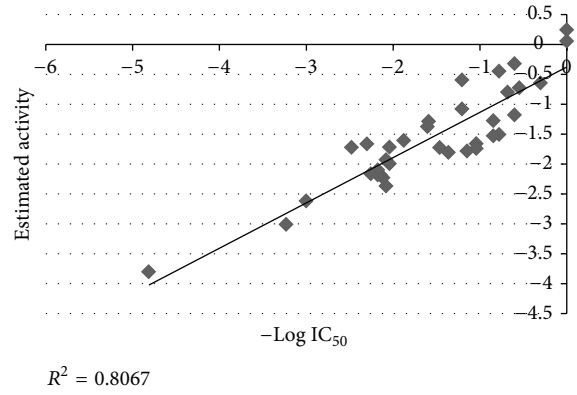

Figure 3: Graph plotted between the actual and estimated activity of training set of compounds.

95% confidence level, and 19 spreadsheets were generated by CatScramble.

2.5. Activity Prediction of Internal and External Test Sets. Test set validation was performed to evaluate the prediction performance of the generated pharmacophore model. An internal test set of 9 compounds from the same chemical series, not involved in the training set, was selected to validate the best pharmacophore model. Moreover, the selected model was also validated using an external test set of 15 compounds taken from a different chemical series having diverse structures [19]. The reason behind this was to test the prediction ability of the model in a wide molecular domain where the external molecules are not similar to the training set molecules.

The test set molecules were built and energy minimized and their conformational analysis was done similar to the training set. The pharmacophore mapping protocol was applied which uses catalyst to identify ligands that map to a pharmacophore and aligns the ligands to the query. Only the best mapping for each ligand was allowed. The squared correlation coefficient (r^2) was obtained by plotting the actual versus estimated activities of the test set compounds.

Table 2: Statistical values and features for the top 10 hypotheses.

Hypotheses	Total cost	Cost difference (null-total cost)	RMSD	Correlation	Features
1	150.914	39.69	0.88645	0.902269	HBA_L, HY, 2RA
2	157.651	32.953	1.10718	0.840131	HBA_L, HY, 2RA
3	173.856	16.748	1.42113	0.727559	HBA_L, HY, 2RA
4	174.987	15.617	1.48308	0.688064	HBA_L, HY, 2RA
5	176.221	14.383	1.46284	0.7101	HBA_L, HY, 2RA
6	179.14	11.464	1.56714	0.640751	HBA_L, HY, 2RA
7	180.984	9.62	1.60018	0.620886	HBA_L, HY, 2RA
8	181.365	9.239	1.6061	0.617387	HBA_L, HY, 2RA
9	182.587	8.017	1.62925	0.602328	HBA_L, HY, 2RA
10	183.831	6.773	1.64821	0.590495	HBA_L, HY, 2RA

Table 3: Actual and predicted activity of the training set compounds.

Compound	Actual activity IC_{50} (nM)	Estimated activity IC_{50} (nM)	Error factor	Actual activity scale[a]	Estimated activity scale[a]
2	1000	412.936	2.5	++	++
3	150	152.223	1.1	++	++
(R,R)-5a	150	125.466	1.1	++	++
(R,S)-5a	130	169.677	1.3	++	++
5b	180	145.506	1.2	++	++
5c	300	52.491	5.8	++	++
5d	120	233.097	2	++	++
5e	75	40.229	1.8	++	++
5f	110	52.049	2.1	++	++
5g	120	84.516	1.4	++	++
5h	200	45.893	4.2	++	++
(R,R)-5j	29	52.876	1.9	++	++
5l	65000	6367.91	10	+	+
5m	110	98.469	1.1	++	++
5n	1700	1024.84	1.6	+	+
6a	40	23.728	1.7	++	++
6c	4.8	6.249	1.3	+++	+++
6d	3.5	5.287	1.6	+++	+++
6f	11	45.567	4.2	++	++
6g	11	55.014	5.1	++	++
6i	14	60.575	4.4	++	++
6j	140	151.456	1.1	++	++
7a	1	0.569	1.6	+++	+++
7c	7	18.834	2.9	+++	++
7d	6	2.788	2.1	+++	+++
7e	7	33.676	4.9	+++	++
7f	39	19.228	2	++	++
7g	16	3.911	4.1	++	+++
7h	2	4.414	2.3	+++	+++
7j	4	2.086	1.9	+++	+++
7k	16	11.999	1.2	++	++
7l	6	31.869	5.4	+++	++
7m	23	63.915	2.8	++	++
7n	1	0.879	1.1	+++	+++
7o	4	15.03	1.5	+++	++

[a]Activity scale: highly active (<10 nM, +++), moderately active (10–1000 nM, ++), and inactive (>1000 nM, +).

Table 4: Validation of the Hypo 1 using the CatScramble program.

Validation number	Total cost	Correlation (r)
Hypo 1	150.914	0.902269
Random trial_1	163.254	0.813374
Random trial_2	156.284	0.869499
Random trial_3	162.449	0.784895
Random trial_4	171.6	0.734126
Random trial_5	159.198	0.828584
Random trial_6	158.681	0.842351
Random trial_7	157.007	0.879218
Random trial_8	166.79	0.766941
Random trial_9	162.874	0.793253
Random trial_10	165.053	0.788512
Random trial_11	156.552	0.861163
Random trial_12	169.679	0.738177
Random trial_13	171.276	0.736358
Random trial_14	153.222	0.873299
Random trial_15	156.565	0.890657
Random trial_16	156.905	0.85654
Random trial_17	166.072	0.771533
Random trial_18	179.171	0.655302
Random trial_19	164.899	0.776163

Table 5: Actual and predicted activities of internal and external test sets based on the best pharmacophore hypothesis Hypo 1.

Compound	Actual activity IC_{50} (nM)	Estimated activity IC_{50} (nM)	Error factor	Actual activity scale[a]	Estimated activity scale[a]
(R)-4	84	394.107	4.7	++	++
(S)-4	490	394.107	1.2	++	++
5i	200	293.232	1.5	++	++
(R,S)-5j	69	354.464	5.1	++	++
6b	16	17.431	1.1	++	++
6e	20	110.752	5.5	++	++
6h*	11	1057.79	96.2	++	+
7b	3	5.506	1.8	+++	+++
7i	13	2.797	4.6	++	+++
		External test set			
3a	7100	6835.94	1.1	+	+
3b	24000	6404.1	3.7	+	+
3c	43000	6560.66	6.5	+	+
3d	12000	6460.16	1.8	+	+
3e	9100	6349.46	1.4	+	+
12a	2500	6454.92	2.6	+	+
12b	600	835.427	1.4	++	++
12c	400	688.096	1.7	++	++
12d	520	508.003	1	++	++
12e	330	709.005	2.1	++	++
12f	210	6651.93	31.7	++	+
12g	53	86.082	1.6	++	++
12h	100	820.03	8.2	++	++
12i	10	288.67	28.9	++	++
12j	1900	671.84	2.8	+	++

*Outlier from the test set compounds.
[a]Activity scale: highly active (<10 nM, +++), moderately active (10–1000 nM, ++), and inactive (>1000 nM, +).

2.6. External Validation with Advanced UT Antagonists. As an additional approach to external validation, some advanced UT antagonists (Figure 1) obtained from the literature [4, 20–23] were mapped on the obtained pharmacophore model. Mapping of these compounds with Hypo 1 was studied for the number of features mapped and fit values.

2.7. Virtual Screening with Sequential Filters. The validated pharmacophore model was applied as a 3D query tool to screen the Maybridge chemical database consisting of over 56,000 organic compounds to retrieve new chemical entities as potent UT antagonists. The virtual screening was performed using the Fast/Flexible search option of DS Catalyst to retrieve putative compounds having their chemical moieties spatially mapped with corresponding features in the pharmacophoric query. Sequential computational filters were applied to find out the best compounds from such a large pool of compounds.

The compounds were first filtered by Lipinski's "rule of five" that sets the criteria for drug-like properties. According to this rule, poor absorption is expected if molecular weight >500, log P > 5, hydrogen bond donors > 5, and hydrogen bond acceptors > 10 [24]. Compounds violating more than one of these rules may not have appropriate bioavailability. [25].

Secondly, the molecules that satisfied all the features of the pharmacophore model used as the 3D query in database searching were retained as hits. This was done on the basis of fit values. Conformational analysis using the "Best" conformation generation method was performed. The "ligand pharmacophore mapping" protocol was applied to map the hits onto the pharmacophores. The fit values were calculated on the basis of the chemical substructures matching to the location constraints of the pharmacophoric features and their distance deviation from the feature centers. High fit values signify good matches. In addition to this the database compounds were also selected on the basis of the estimated values. The flowchart in Figure 2 is a schematic representation of the sequential filters for virtual screening.

3. Results and Discussion

3.1. Statistical Assessment of Pharmacophore Model. The HypoGen algorithm [26] implemented in Discovery Studio generated ten pharmacophore hypotheses using all the information related to conformational models and chemical features of 35 training set compounds. The fixed cost of the 10 top-scored hypotheses was 136.081 bits, and the null hypothesis cost was 190.604 bits. A difference of 54 bits between null and fixed costs signified the predictive nature of the hypotheses. The first hypothesis (Hypo1) consisting of four features, one HBA_L, one HY, and two RA, was considered as the best pharmacophore model, on the basis of high correlation coefficient, high cost difference, and low RMSD (Table 2).

The total cost of Hypo 1 (150.914) and the large difference between null and total cost (D_{cost} = 39.69) coupled with a high correlation coefficient (r = 0.902) and a low RMSD

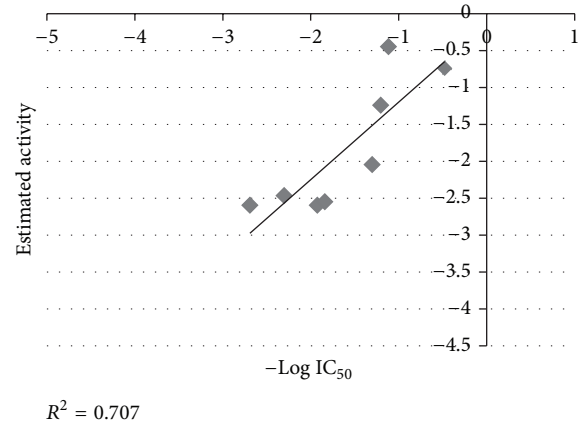

Figure 4: Graph plotted between the actual and estimated activity of internal test set of compounds.

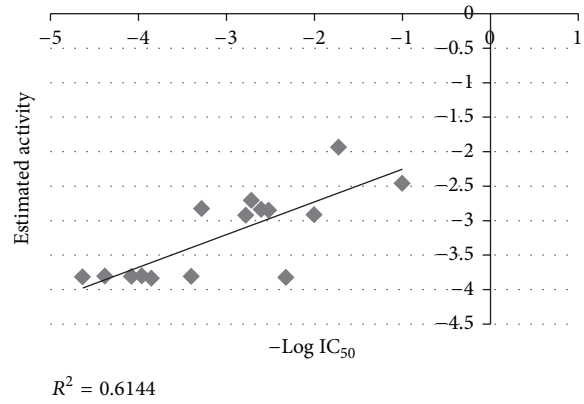

Figure 5: Graph plotted between the actual and estimated activity of external test set of compounds.

(0.886) ensured that a true correlation had been established in the model. Moreover, the cost difference between total and fixed costs for the best hypothesis was only 14.833 bits, indicating the high probability of the true correlation of the data. The configuration cost (17.286) of the hypothesis slightly exceeded the limit of 17 bits but can be accepted as the model meets the other criteria of validation [27].

Highly validated and statistically perfect pharmacophore model (Hypo1) was used to predict the activity of training set compounds. All the compounds were classified in the activity scale of highly active (<10 nM, +++), moderately active (10–1000 nM, ++), and inactive (>1000 nM, +). Among the 35 training set compounds, four highly active compounds were predicted as moderately active and one moderately active compound was predicted as highly active. Consequently, for 30 out of 35 training set compounds, the predicted activity values were within the same activity scale as the experimental values.

Table 3 represents the actual and predicted activities of the training set based on the best pharmacophore hypothesis. Figure 3 shows the graph plotted between the actual and

Table 6: Interfeature distances (in Å) between the obtained pharmacophore features[a].

	RA1 (IP1)	RA1 (PP1)	RA2 (IP2)	RA2 (PP2)	HBA_L (IP)	HBA_L (PP)
RA1 (IP1)						
RA1 (PP1)	3.000					
RA2 (IP2)	7.059	8.058				
RA2 (PP2)	8.058	9.524	3.000			
HBA_L (IP)	6.223	7.032	6.993	9.194		
HBA_L (PP)	6.679	8.385	5.635	8.278	3.000	
HY	9.683	10.795	3.615	4.774	7.120	5.263

[a]IP: initial point in the ligand and PP: projected point in the active site of the receptor.

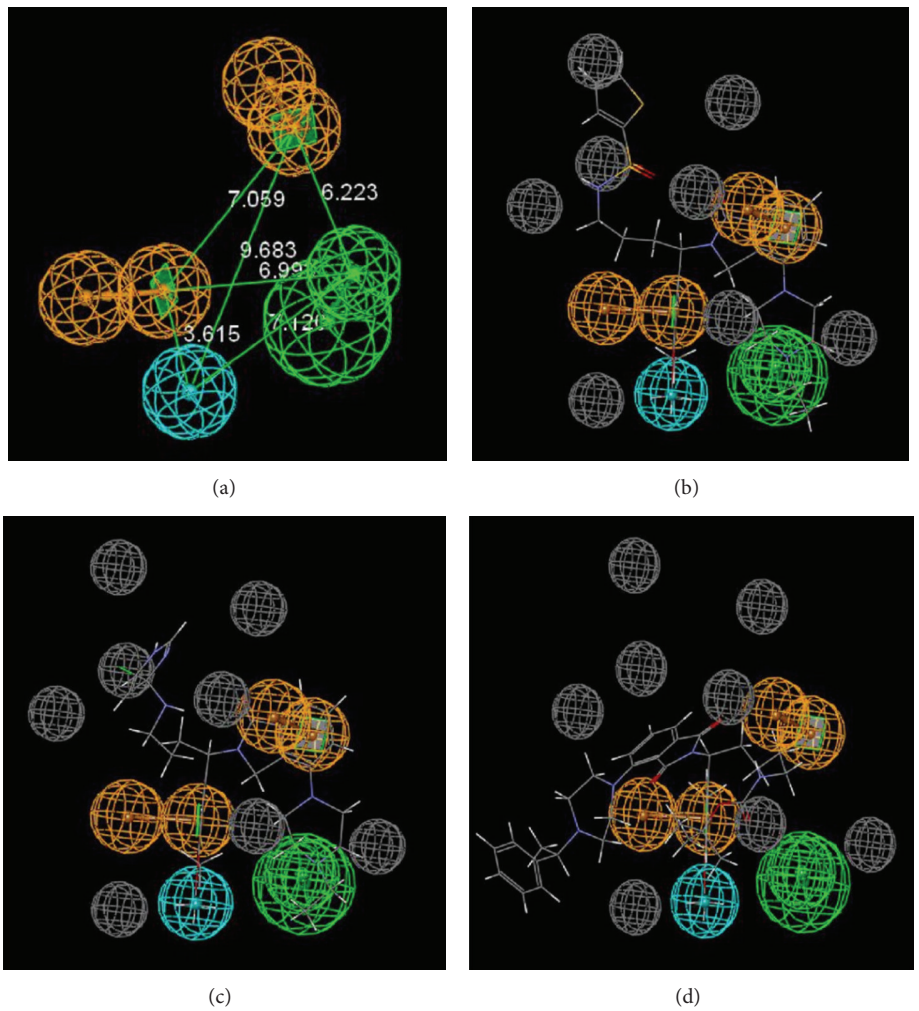

Figure 6: The obtained pharmacophore model (orange: RA, green: HBA_L, blue: HY, and grey: excluded volumes) showing (a) interfeature distances, (b) mapping of one of the most potent compounds, 7a, (c) mapping of the other most potent compound, 7n, and (d) mapping of the least active compound 5l.

estimated activities of training set compounds, as predicted by Hypo 1.

3.2. CatScramble Validation. The CatScramble method based on the principle of Fisher's randomization test was used to evaluate the statistical significance of the pharmacophore hypotheses generated from the training set molecules. To achieve a confidence level of 95%, 19 random spreadsheets (random hypotheses) were generated amongst the molecules of the training set. The data of cross validation provided

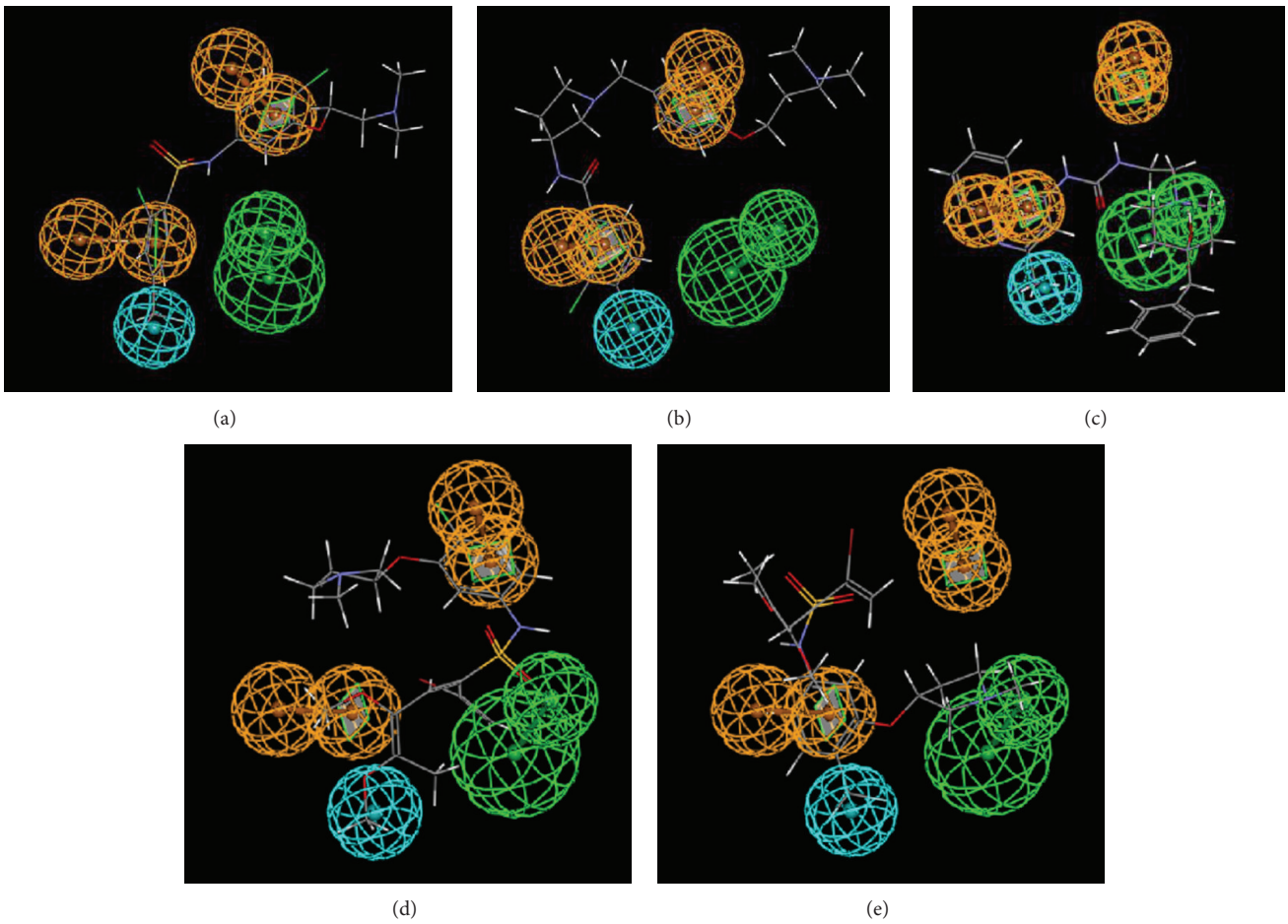

Figure 7: Mapping of advanced UT antagonists on the obtained pharmacophore model; (a) SB-611812 (fit value: 6.811), (b) SB-657510 (fit value: 6.505), (c) palosuran (Fit value: 5.714), (d) SB-706375 (fit value: 5.555), and (e) SB-436811 (Fit value: 5.334).

confidence that the Hypo1 was not generated by chance, as indicated by the better statistical values (lowest total cost and highest correlation coefficient) of Hypo 1 (Table 4).

3.3. Activity Prediction of Internal and External Test Sets. The model was subjected to test set validation to find out how correctly the model predicts the activity of the test set molecules. Out of the 9 internal test set compounds, one compound showed a high error ratio of 96.2, suggesting that this compound might be a potential outlier (Table 5). Its removal significantly improved the r^2 (0.707) between the actual and estimated activities of the test set (Figure 4). This clearly demonstrated that the pharmacophore model has the ability to predict the activity of new compounds with high efficiency.

The selected pharmacophore was further validated using an external set of phenylpiperidine-benzoxazinones-based 15 molecules with UT antagonist activity [19]. The activities of all the external test set compounds were estimated using Hypo 1 (Table 5). The squared correlation coefficient value of 0.614 testified the prognostic nature of the developed pharmacophore model (Figure 5). This validation gave an added confidence in the usability of the selected pharmacophore.

3.4. Pharmacophore Mapping Analysis. The pharmacophore features (1HBA_L, 2RA, and 1HY) and their interfeature distances are given in Figure 6(a) and Table 6. The two most active compounds 7a and 7n are mapped very well with all the four pharmacophore features (Figures 6(b) and 6(c)). The pharmacophore mapping reveals that the basic piperazine nitrogen having ethyl group (R^2) is mapped to the HBA_L feature and phthalimide and isoindolinone benzene ring is mapped to one RA whereas the dimethoxybenzene ring is mapped to the other RA feature. The HY feature is mapped with one of the methoxy group of dimethoxybenzene. The least active compound 5l is mapped only with two features (1RA and 1HY) out of four, missing 1RA and 1HBA_L (Figure 6(d)). The pharmacophore mapping analysis discloses the importance of the main scaffold towards antagonist activity. Nevertheless, the N-alkyl groups at R^2 position are important for the basicity of the piperazine nitrogen. Ethyl has been the most favourable N-alkyl group for antagonist activity. On the other hand, bulkier N-alkyl substitutions creating steric hindrance are not favourable for activity. The pharmacophore mapping shows that R^1 substitutions are not playing an important role in the drug-receptor interaction which is evident by the presence of some

Table 7: Hits obtained from pharmacophore-based Maybridge chemical compound database screening.

Name of compounds	Estimated activity	Fit value	Chemical structure
AW 00785	9.1108	7.6404	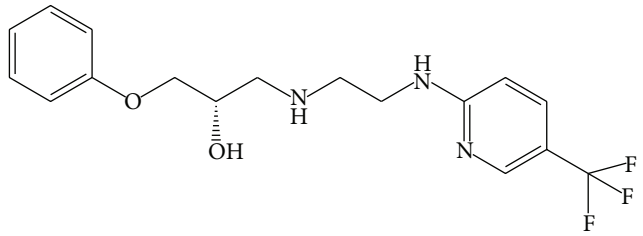
DSHS 00776	9.7235	7.6122	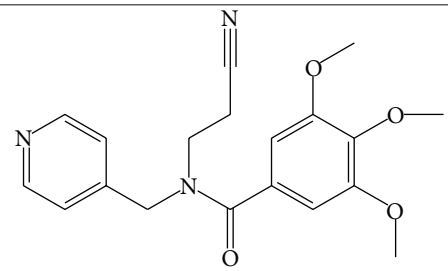
HTS 04602	48.9014	6.9107	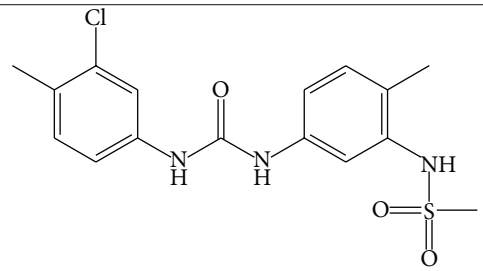
BTB 02340	63.3128	6.7985	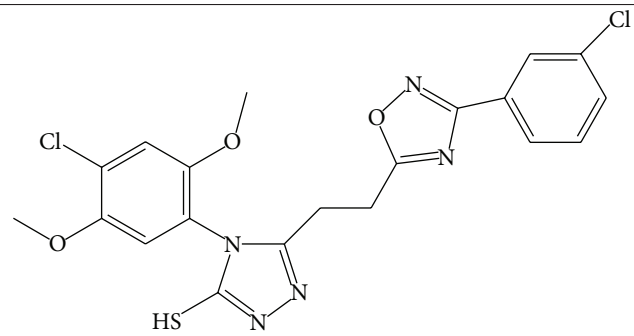
KM 04691	68.793	6.7625	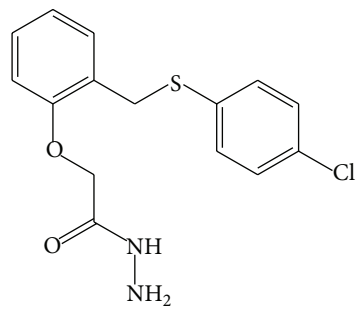

excluded volumes at this position (Figures 6(b) and 6(c)). Moreover, the conformationally constrained scaffold having less conformational freedom is important for activity.

3.5. Mapping with Advanced UT Antagonists. As an additional validation step, some of the chemically diverse advanced UT antagonist drug candidates like palosuran, SB-611812, SB-657510, SB-706375, and SB-436811 [4, 20–23] were mapped on the developed pharmacophore. All five compounds showed three-feature mapping with good fit values (Figure 7). SB-611812 and SB-657510 mapped with two RA and one HY, missing the HBA_L feature. Whereas SB-706375, SB-436811, and palosuran mapped well with one RA, one HY, and one HBA_L, thus missing one RA feature. SB-611812 showed the maximum fit value of 6.811.

3.6. Virtual Screening. A total of 298 compounds were retrieved as hits from virtual screening of Maybridge database. These compounds were first screened for drug-like properties using Lipinski's rule of 5 as filter. 230 compounds that passed the screening were overlaid with the best 3D pharmacophore model (Hypo1) by using the "Best Fit" selection. Out of these, 20 compounds had an estimated activity within the range of 1–1000 nM and fit value >5.5. The best 5 compounds having estimated activity (nM) in single and double digits are reported in Table 7.

4. Conclusions

In view of the potential of UT antagonists as novel cardiovascular agents, we attempted to develop a 3D pharmacophore model to evaluate the structural requirements for potent UT antagonists. The developed pharmacophore model was validated with multiple methods. The results demonstrate that one hydrogen bond acceptor lipid (HBA_L) and two ring aromatic (RA) and one hydrophobic (HY) features contribute significantly towards the antagonist activity. The pharmacophore model was used for screening the Maybridge chemical database to identify new compounds as UT antagonists. This pharmacophore model provides stringent structural requirements along with interfeature distances and can be further used for the design and development of novel UT antagonists.

Conflict of Interests

The authors declare that they have no conflict of interests.

Acknowledgment

The authors would like to thank the Vice Chancellor, Banasthali University, for extending all the necessary facilities.

References

[1] R. S. Ames, H. M. Sarau, J. K. Chambers et al., "Human urotensin-II is a potent vasoconstrictor and agonist for the orphan receptor GPR14," *Nature*, vol. 401, no. 6750, pp. 282–286, 1999.

[2] C. D. Proulx, B. J. Holleran, P. Lavigne, E. Escher, G. Guillemette, and R. Leduc, "Biological properties and functional determinants of the urotensin II receptor," *Peptides*, vol. 29, no. 5, pp. 691–699, 2008.

[3] B. E. Maryanoff and W. A. Kinney, "Urotensin-II receptor modulators as potential drugs," *Journal of Medicinal Chemistry*, vol. 53, no. 7, pp. 2695–2708, 2010.

[4] M. Clozel, P. Hess, C. Qiu, S.-S. Ding, and M. Rey, "The urotensin-II receptor antagonist palosuran improves pancreatic and renal function in diabetic rats," *Journal of Pharmacology and Experimental Therapeutics*, vol. 316, no. 3, pp. 1115–1121, 2006.

[5] "Actelion provides update on palosuran in diabetic nephropathy," http://www1.actelion.com/en/our-company/news-and-events/index.page?newsId=1209557.

[6] P. J. Lakshmi, B. V. S. Kumar, R. S. Nayana et al., "Design, synthesis, and discovery of novel non-peptide inhibitor of Caspase-3 using ligand based and structure based virtual screening approach," *Bioorganic and Medicinal Chemistry*, vol. 17, no. 16, pp. 6040–6047, 2009.

[7] S. Sundriyal, R. K. Sharma, R. Jain, and P. V. Bharatam, "Minimum requirements of hydrophobic and hydrophilic features in cationic peptide antibiotics (CPAs): pharmacophore generation and validation with cationic steroid antibiotics (CSAs)," *Journal of Molecular Modeling*, vol. 14, no. 4, pp. 265–278, 2008.

[8] S. Paliwal, M. Pal, D. Yadav, S. Singh, and R. Yadav, "Ligand-based drug design studies using predictive pharmacophore model generation on 4H-1,2,4-triazoles as AT1 receptor antagonists," *Medicinal Chemistry Research*, vol. 21, no. 9, pp. 2307–2315, 2012.

[9] C. Lu, F. Jin, C. Li, W. Li, G. Liu, and Y. Tang, "Insights into binding modes of 5-HT2c receptor antagonists with ligand-based and receptor-based methods," *Journal of Molecular Modeling*, vol. 17, no. 10, pp. 2513–2523, 2011.

[10] K. K. Roy, S. Singh, and A. K. Saxena, "Integration-mediated prediction enrichment of Quantitative model for Hsp90 inhibitors as anti-cancer agents: 3D-QSAR study," *Molecular Diversity*, vol. 15, no. 2, pp. 477–489, 2011.

[11] D. Yadav, S. Paliwal, R. Yadav, M. Pal, and A. Pandey, "Identification of novel HIV 1-protease inhibitors: application of ligand and structure based pharmacophore mapping and virtual screening," *PLoS ONE*, vol. 7, no. 11, Article ID e48942, 2012.

[12] E. Lescot, J. S. O. Santos, C. Dubessy et al., "Definition of new pharmacophores for nonpeptide antagonists of human urotensin-II. Comparison with the 3D-structure of human urotensin-II and URP," *Journal of Chemical Information and Modeling*, vol. 47, no. 2, pp. 602–612, 2007.

[13] E. Lescot, J. S. O. Santos, N. Colloc'h et al., "Three-dimensional model of the human urotensin-II receptor: docking of human urotensin-II and nonpeptide antagonists in the binding site and comparison with an antagonist pharmacophore model," *Proteins*, vol. 73, no. 1, pp. 173–184, 2008.

[14] E. C. Lawson, D. K. Luci, S. Ghosh et al., "Nonpeptide urotensin-II receptor antagonists: a new ligand class based on piperazino-phthalimide and piperazino-isoindolinone subunits," *Journal of Medicinal Chemistry*, vol. 52, no. 23, pp. 7432–7445, 2009.

[15] T. Langer and R. D. Hoffmann, "Pharmacophore model generation software tools," in *Pharmacophores and Pharmacophores Searches*, Methods and Principles in Medicinal Chemistry, pp. 17–44, Wiley-VCH, Weinheim, Germany, 2006.

[16] K. S. Watts, P. Dalal, R. B. Murphy, W. Sherman, R. A. Friesner, and J. C. Shelley, "ConfGen: a conformational search method for efficient generation of bioactive conformers," *Journal of Chemical Information and Modeling*, vol. 50, no. 4, pp. 534–546, 2010.

[17] A. Smellie, S. L. Teig, and P. Towbin, "Poling: promoting conformational variation," *Journal of Computational Chemistry*, vol. 16, no. 2, pp. 171–187, 1995.

[18] M. Tonelli, V. Boido, P. L. Colla et al., "Pharmacophore modeling, resistant mutant isolation, docking, and MM-PBSA analysis: combined experimental/computer-assisted approaches to identify new inhibitors of the bovine viral diarrhea virus (BVDV)," *Bioorganic and Medicinal Chemistry*, vol. 18, no. 6, pp. 2304–2316, 2010.

[19] D. K. Luci, S. Ghosh, C. E. Smith et al., "Phenylpiperidine-benzoxazinones as urotensin-II receptor antagonists: synthesis, SAR, and in vivo assessment," *Bioorganic and Medicinal Chemistry Letters*, vol. 17, no. 23, pp. 6489–6492, 2007.

[20] N. Bousette, F. Hu, E. H. Ohlstein, D. Dhanak, S. A. Douglas, and A. Giaid, "Urotensin-II blockade with SB-611812 attenuates cardiac dysfunction in a rat model of coronary artery ligation," *Journal of Molecular and Cellular Cardiology*, vol. 41, no. 2, pp. 285–295, 2006.

[21] S. A. Douglas, D. J. Behm, N. V. Aiyar et al., "Nonpeptidic urotensin-II receptor antagonists I: in vitro pharmacological characterization of SB-706375," *The British Journal of Pharmacology*, vol. 145, no. 5, pp. 620–635, 2005.

[22] J. Jin, D. Dhanak, S. D. Knight et al., "Aminoalkoxybenzyl pyrrolidines as novel human urotensin-II receptor antagonists," *Bioorganic and Medicinal Chemistry Letters*, vol. 15, no. 13, pp. 3229–3232, 2005.

[23] J. Jin, M. An, A. Sapienza et al., "Urotensin-II receptor antagonists: synthesis and SAR of N-cyclic azaalkyl benzamides," *Bioorganic and Medicinal Chemistry Letters*, vol. 18, no. 14, pp. 3950–3954, 2008.

[24] C. A. Lipinski, "Drug-like properties and the causes of poor solubility and poor permeability," *Journal of Pharmacological and Toxicological Methods*, vol. 44, no. 1, pp. 235–249, 2000.

[25] I. Muegge, "Selection criteria for drug-like compounds," *Medicinal Research Reviews*, vol. 23, no. 3, pp. 302–321, 2003.

[26] O. F. Güner, "HypoGen: an automated system for generating 3D predictive pharmacophore models," in *Pharmacophore Perception, Development, and Use in Drug Design*, IUL Biotechnology Series, pp. 171–189, International University Line, La Jolla, Calif, USA, 2000.

[27] M. Pal and S. Paliwal, "In silico identification of novel lead compounds with AT1 receptor antagonist activity: successful application of chemical database screening protocol," *Organic and Medicinal Chemistry Letters*, vol. 2, no. 1, article 7, 2012.